Subterranean Karst Environments as a Global Sink for Atmospheric Methane

Kevin D. Webster[1,2,*], Agnieszka Drobniak[3], Giuseppe Etiope[4,5], Maria Mastalerz[3], Peter E. Sauer[6], Arndt Schimmelmann[6]

[1]School of Natural Resources and the Environment, University of Arizona, 1064 E Lowell St, Tucson, Arizona 85721, USA

[2]Department of Ecology and Evolutionary Biology, University of Arizona, 1041 E Lowell St, Tucson, Arizona 85721, USA.

[3]Indiana Geological Survey, Indiana University, 611 North Walnut Grove Ave., Bloomington, Indiana 47405, USA.

[4] Istituto Nazionale di Geofisica e Vulcanologia, Sezione Roma 2, Italy.

[5] Faculty of Environmental Science and Engineering, Babes-Bolyai University, Cluj-Napoca, Romania.

[6] Department of Earth and Atmospheric Sciences, Indiana University, 1001 E 10th St. Bloomington, IN 47405, USA.

* corresponding author: kevdwebs@email.arizona.edu; telephone: 520-621-2539.

Abstract: The air in subterranean karst cavities is often depleted in methane (CH_4) relative to the atmosphere. Karst is considered a potential sink for the atmospheric greenhouse gas CH_4 because its subsurface drainage networks and solution-enlarged fractures facilitate atmospheric exchange. Karst landscapes cover about 14 % of earth's continental surface, but observations of CH_4 concentrations in cave air are limited to localized studies in Gibraltar, Spain, Indiana (USA), Vietnam, Australia, and by incomplete isotopic data. To test if karst is systematically acting as a global CH_4 sink, we measured the CH_4 concentrations, $\delta^{13}C_{CH_4}$, and $\delta^2H_{CH_4}$ values of cave air from 33 caves in the USA and three caves in New Zealand. We also measured CO_2 concentrations, $\delta^{13}C_{CO_2}$, and radon (Rn) concentrations to support CH_4 data interpretation by assessing cave air residence times and mixing processes. Among these caves, 35 exhibited subatmospheric CH_4 concentrations in at least one location compared to their local atmospheric backgrounds. CH_4 concentrations and $\delta^{13}C_{CH_4}$ and $\delta^2H_{CH_4}$ values suggest that microbial methanotrophy within caves is the primary CH_4 consumption mechanism as the atmosphere exchanges with subsurface air. The pattern of $\delta^{13}C_{CH_4}$ and $\delta^2H_{CH_4}$ values along CH_4 concentration gradients in cave air provides evidence for incomplete oxidation by methanotrophy. Only 5 locations from 3 caves showed elevated CH_4 concentrations compared to the atmospheric background and could be ascribed to local CH_4 sources from sewage and outgassing swamp water. Several associated $\delta^{13}C_{CH_4}$ and $\delta^2H_{CH_4}$ values point to carbonate reduction and acetate fermentation as biochemical pathways of limited methanogenesis in karst environments and suggest that these pathways occur in the environment over large spatial scales. Our data show that karst environments function as a global CH_4 sink. Estimates of CH_4 flux in karst landscapes are needed in order to include the subterranean CH_4 sink in climate models.

Keywords: cave; greenhouse gas; karst; methane; methanogenesis; methanotrophy

1

1. Introduction

Atmospheric methane (CH_4) is a greenhouse gas and its concentration is increasing in the atmosphere (Dlugokencky et al., 2011; Sussmann et al., 2012; Ciais et al., 2013). The increase in atmospheric CH_4 is due to an imbalance between CH_4 sources and sinks. Anthropogenic and natural sources combine to contribute about 680 Tg of CH_4 to the atmosphere while reactions with hydroxyl ($\cdot OH$) and chlorine radicals in the troposphere and stratosphere remove about 600 Tg a^{-1} (Kirschke et al., 2013). Methanotrophic consumption in soils removes 30 Tg a^{-1} (Kirschke et al., 2013). The present globally averaged CH_4 concentration is 1.87 ppmv which is 2.5 times higher than preindustrial levels (Nisbet et al., 2016). Despite improvements in estimating individual sources and sinks of atmospheric CH_4, the associated errors remain large (Kirschke et al., 2013). Recent studies suggest that caves may act as an additional CH_4 sink (Mattey et al., 2013; Fernandez-Cortes et al., 2015; McDonough et al., 2016; Webster et al., 2016; Lennon et al., 2017).

Caves and associated karst landscapes may be an important overlooked sink for atmospheric CH_4 because they are estimated to cover as much as 10 to 20 % of the continental surface with the more precise estimates suggesting about 13.8 % (Palmer, 1991; Ford and Williams, 2007). Karst landscapes are frequently associated with the chemical dissolution of limestones, but can form in any soluble rock body. The resulting caves, solution-enlarged fractures, and internal drainage networks that function to transport mass from high elevations to low elevations also allow for subsurface-surface atmospheric exchange (Kowalczk and Froelich, 2010; Garcia-Anton et al., 2014). The total volume and surface area of karst conduits able to interact with the atmosphere is unknown, in part due to small fractures and the difficulty of imaging the subsurface with geophysical methods. Karst caves, due to their accessibility, provide opportunities for non-invasive, *in-situ* analyses and sampling.

Cave and karst landscapes form in two common ways, each of which influences karst's capacity to act as a CH_4 sink. Epigenic karst forms through the interaction of limestone with carbonic acid derived from the dissolution of atmospheric and soil CO_2 into surface waters, and hypogenic caves form when corrosive water from deep sources migrates into and dissolves limestone bedrock. Epigenic caves are more widespread, and atmospheric to subatmospheric CH_4 concentrations of 1.8 ppmv to < 0.1 ppmv have been observed in these settings (Mattey et al., 2013; Fernandez-Cortes et al., 2015; McDonough et al., 2016; Webster et al., 2016; Lennon et al., 2017). In some hypogenic caves be contrast, elevated CH_4 concentrations from 2 ppmv to 1 % have been observed in association with CH_4-rich springs or seeps related to fluid migration from deep hydrocarbon-bearing sedimentary rocks, i.e. seepage processes that are widespread on Earth (Sarbu et al., 1996; Hutchens et al., 2004; Jones et al., 2012; Webster et al., 2017). The dominance of epigenic karst suggests that karst is likely functioning as a CH_4 sink at the global scale, but more observations are needed.

Different hypotheses have been put forward to explain the low CH_4 concentrations observed in epigenic cave air. The combination of subatmospheric CH_4 concentrations and the stable carbon isotopic ratio of CH_4 in the air of caves in Gibraltar led to the hypothesis that microorganisms were responsible for the removal of CH_4 (Mattey et al., 2013). In turn, low CH_4 concentrations in Spanish caves, in the presumed absence of CH_4-consuming (methanotrophic) bacteria, led to the hypothesis that CH_4 oxidation was induced by ions and $\cdot OH$ generated by the radioactive decay of radon and daughter nuclides (Fernandez-Cortes et al., 2015). Since these initial observations, datasets from caves in Australia, the USA, and Vietnam have pointed towards methanotrophic CH_4 oxidation (McDonough et al., 2016; Webster et al., 2016; Lennon et al., 2017).

The chemical composition of cave air results from the mixing of the atmosphere and air from the overlying soils and epikarst and these processes should influence the CH_4 concentrations of cave air. Previous studies have shown that CH_4 concentrations have been inversely correlated with CO_2 concentrations in cave air (Mattey et al., 2013; Ferndandez-Cortes et al., 2015; McDonough et al., 2016;

Webster et al., 2016). Cave air CO_2 concentrations are positively correlated with radon (Rn) concentrations and Rn is known to track cave air residence time (Cunningham and LaRock, 1991; Batiot-Guilhe et al., 2007; Kowalczk and Froelich, 2010; Mattey et al., 2010; Gregorič et al., 2011, 2014). Additionally, the stable C isotope composition of CO_2 ($\delta^{13}C_{CO_2}$), can track the sources of CO_2 in the environment. For example, $\delta^{13}C_{CO_2}$ values of −24 ‰ are associated with soil CO_2, while atmospheric CO_2 has $\delta^{13}C_{CO_2}$ values ranging from −8.5 ‰ to −10 ‰ (Amundson et al., 1998; Keeling et al., 2010; Peyraube et al., 2013). Thus CO_2, Rn, and $\delta^{13}C_{CO_2}$ in cave air can help determine the influence of cave air mixing processes on CH_4.

The stable C and H isotope compositions of CH_4 ($\delta^{13}C_{CH_4}$ and $\delta^{2}H_{CH_4}$) also provide tools for understanding the sources and sinks of CH_4 in caves because different CH_4 sources are associated with characteristic $\delta^{13}C_{CH_4}$ and $\delta^{2}H_{CH_4}$ values. For example, CH_4 produced from carbonate reduction has $\delta^{13}C_{CH_4}$ and $\delta^{2}H_{CH_4}$ values that range from −112 to −60 ‰ VPDB and from −350 to −100 ‰ VSMOW respectively (Whiticar, 1999), and atmospheric CH_4 has $\delta^{13}C_{CH_4}$ and $\delta^{2}H_{CH_4}$ values around −47.5 and −100 ‰ (Miller et al., 2002; Townsend-Small et al., 2012). The $\delta^{13}C_{CH_4}$ and $\delta^{2}H_{CH_4}$ values of CH_4 can also be altered through secondary processes such as oxidation and mixing. The oxidation pathways of CH_4 by methanotrophs or ·OH have fractionation factors that result in residual CH_4 having increased in $\delta^{2}H_{CH_4}$ values of 8.5 ‰ for every 1 ‰ increase in $\delta^{13}C_{CH_4}$ value and increases in $\delta^{2}H_{CH_4}$ values of 72 ‰ for every 1 ‰ increase in $\delta^{13}C_{CH_4}$ value, respectively (Feisthauer et al., 2011; Saueressig et al., 2001). Mixing between two different CH_4 sources creates a linear trend between the two members. Thus measuring the $\delta^{13}C_{CH_4}$ and $\delta^{2}H_{CH_4}$ of cave air should allow for the determination of cave air CH_4 sources.

The objective of the present work is to extend the karst CH_4 dataset and test the hypothesis that karst systems act as a CH_4 sink on a global scale. To this aim, we studied CH_4 concentration, $\delta^{13}C_{CH_4}$, and $\delta^{2}H_{CH_4}$ in cave air from 33 epigenic caves in the USA and three epigenic caves in New Zealand. CO_2, $\delta^{13}C_{CO_2}$, and Rn were also measured to support CH_4 data interpretation *via* assessing cave air residence times and mixing processes. Data analysis is focused on determining CH_4 concentrations, origin, mixing processes and isotopic fractionations.

2. Methods

2.1. Sampling and analyses

Air samples from 16 limestone or dolostone caves in the Appalachian fold and thrust belt, 17 limestone caves in gently warped intracratonic basins of the USA, and 3 caves from the North Island of New Zealand were collected over a timespan of roughly four years (Fig. 1; Table 1). Cave air was analyzed using *in-situ* methods and was further sampled for laboratory analysis. *In-situ* CH_4, CO_2, and Rn abundance analyses were carried out using a suite of instruments (Table 2). Discrete samples of cave air were collected in pre-evacuated 50-mL serum vials, in 1 to 3-L Tedlar® bags, or in 4-L glass bottles. CH_4 and CO_2 concentrations of discrete samples were measured *via* gas chromatography.

We assessed cave air mixing processes through the following techniques. A qualitative estimate on cave air residence time was obtained by comparing CH_4 to CO_2 concentrations at individual locations in each cave. Additionally, we measured the Rn concentrations of caves 32 through 36 to assess the relationship between cave air residence time, CH_4 concentrations, and CO_2 concentrations. $\delta^{13}C_{CO_2}$ data were used to assess the sources of CO_2 and thus of air entering the caves. We also assessed the distance from each sampling location to cave entrances as another tool to understand the sources and sinks of CH_4 in caves.

CH_4 and CO_2 concentrations from discrete air samples were measured at Indiana University using a Varian 450 gas chromatograph (GC) (Varian – Agilent Technologies, Palo Alto, California). The GC was fitted with a flame ionization detector (FID) for CH_4 and a thermal conductivity detector (TCD) for CO_2. Standard gas mixtures from Air Liquide America Specialty Gasses LLC (Plumsteadville, Pennsylvania) were used for 3-point calibration curves to convert signals measured on the GC to concentrations. CH_4 standards measured on the GC had errors of ± 5 to ± 14 % of the reported concentrations. CH_4 concentrations are reported with the uncertainty associated with the standard curve unless the calculated uncertainty was ≤ 0.1 ppmv. Samples with calculated uncertainties ≤ 0.1 ppmv were assigned uncertainties of 0.1 ppmv based on replicate measurements. The uncertainty associated with standard curves for CO_2 concentrations varied from < ± 1 to 5 %. CO_2 concentrations were assigned uncertainties based on their associated standard curve.

The stable carbon isotope ratios of CH_4 and CO_2 and hydrogen stable isotope ratios of CH_4 were measured on a ThermoFinnigan Delta Plus XP mass spectrometer in the Stable Isotope Research Facility at Indiana University. Carbon stable isotope ratios are expressed as conventional $\delta^{13}C_{CH_4}$ and $\delta^{13}C_{CO_2}$ values in ‰ along the scale anchored to Vienna Pee Dee Belemnite (VPDB). Hydrogen stable isotope ratios are expressed as $\delta^2H_{CH_4}$ values in ‰ along the scale anchored to Vienna Standard Mean Ocean Water (VSMOW). CH_4 samples were measured in continuous-flow mode using CH_4 preconcentration, cryofocusing (Miller et al., 2002), and a gas chromatography-oxidation/pyrolysis-isotope ratio mass spectrometer (GC-ox/pyr-IRMS) interface. Varying sample extraction times were used to isolate roughly 0.45 and 0.90 μmol of CH_4 prior to the introduction of the sample to the GC-ox/pyr-IRMS for analysis of $\delta^{13}C_{CH_4}$ and $\delta^2H_{CH_4}$ values, respectively. In-house CH_4 standards methane #3, methane #6, and methane ALM with $\delta^{13}C_{CH_4}$ and $\delta^2H_{CH_4}$ values of [+19.86 ± 0.05; +2.2 ± 1.2] ‰, [−39.40 ± 0.02; −153 ± 2] ‰, and [−58.6 ± 0.03; −272.2 ± 3.4] ‰ were used for 2-point normalizations. Errors associated with $\delta^{13}C_{CH_4}$ and $\delta^2H_{CH_4}$ values were calculated using a standard curve that accounted for the peak size of the measurement. Analytical repeatability of internal standards ranged from 0.14 to 0.6 ‰ for $\delta^{13}C_{CH_4}$ and from to 7 to 18 ‰ for $\delta^2H_{CH_4}$.

$\delta^{13}C_{CO_2}$ values were measured in continuous-flow mode using a GasBench II inlet (Tu et al., 2001). Measured $^{13}C/^{12}C$ ratios of CO_2 from cave air were converted to the VPDB scale using a single isotopically characterized in-house standard that has a value of 12.0 ± 0.2 ‰.

2.2 Data elaboration and quality control

In-situ measurements were preferentially used when statistically analyzing gas concentration data. When *in-situ* measurements were not available, concentrations measured on the GC were used in the statistical analyses. Samples and data were screened for quality control by comparing the samples with *in-situ* measurements and visual estimation of the volume of sample bags. If a sample bag had been shown to exhibit a leak for one analyte, data from that sample were discarded. CH_4 and CO_2 concentrations measured by both GC-FID and FTIR showed strong agreements (GC(CO_2) = 0.92 ± 0.04 * FTIR(CO_2) + 100 ± 300, r^2 = 0.99, p = 5*10^{-19}; GC(CH_4) = 0.7 ± 0.2 * FTIR(CH_4) + 0.2 ± 0.2, r^2 = 0.62), and the stable isotopic composition of the samples was not related to their storage time ($\delta^{13}C_{CH_4}$ = 0.2 ± 0.3*day −47 ± 2, r^2 = 0.03, p = 0.32; $\delta^2H_{CH_4}$ = 0.03 ± 0.14*day −96 ± 11, r^2 = 0.005, p = 0.72; $\delta^{13}C_{CO_2}$ = −0.05 ± 0.16*day −19.9 ± 1.8, r^2 = 0.006, p = 0.57). In locations where more than one sample was taken with *in-situ* methods, the values of the samples were averaged. In total, 199 CH_4 concentrations, 192 CO_2 concentrations, 32 $\delta^{13}C_{CH_4}$ values, 26 $\delta^2H_{CH_4}$ values, and 60 $\delta^{13}C_{CO_2}$ values are reported in this study (Supplemental Tables 1, 2). All samples are reported with 95 % confidence intervals.

4

Two different modeling techniques were used to assess trace gas sources and sinks in the studied caves. Keeling plots were used to assess the possibility of a two end member mixing system affecting $\delta^{13}C_{CO_2}$. The stable isotopic composition of CO_2 entering the caves ($\delta^{13}C_s$) was assessed through equation 1

$$\delta^{13}C_s = (\delta^{13}C_m - F_{atm} * \delta^{13}C_{atm})\,(1 - F_{atm})^{-1} \qquad\qquad (1)$$

where $\delta^{13}C_m$ is the $\delta^{13}C_{CO_2}$ of the sample, $\delta^{13}C_{atm}$ is the $\delta^{13}C_{CO_2}$ of the atmosphere, and F_{atm} is the fraction of atmospheric CO_2 in the CO_2 concentration of the sample (Peyraube et al., 2016). We used values of −10 ‰ for $\delta^{13}C_{atm}$ and 400 ppmv for the concentration of atmospheric CO_2.

Rayleigh distillation models were used as the theoretical basis to examine changes in the stable isotopic composition of CH_4 in cave air caused by methanotrophy or ·OH oxidation. The δ-value of an isotope system in a chemical compound of interest (e.g., CH_4) in cave air can be modeled as

$$\delta_c = (\delta_i + 1000)\, f^{\,(-\alpha + 1)} - 1000 \qquad\qquad (2)$$

where δ_c is the instantaneous δ-value of a particular isotope system in cave air after partial consumption, δ_i is the initial δ-value of the isotope system in cave air, f is the fraction of the compound remaining, and α is the kinetic isotope fractionation factor (Mattey et al., 2013). α values of 1.018 and 1.1353 were used to model changes in $\delta^{13}C_{CH_4}$ and $\delta^2H_{CH_4}$ caused by methanotrophy (Coleman et al., 1981; Feisthauer et al., 2011). α values for changes in $\delta^{13}C_{CH_4}$ caused by methanotophy have been observed to range from 1.003 to 1.039 (Templeton et al., 2006; Feisthauer et al., 2011); 1.018 was selected based on observations of methanotrophy in soils and its similarity to the α value of 1.012 observed in St. Michael's Cave in Gibraltar (Feisthauer et al., 2011; Mattey et al., 2013). α values of 1.0039 and 1.294 were used to model changes in $\delta^{13}C_{CH_4}$ and $\delta^2H_{CH_4}$ values caused by ·OH oxidation (Saueressig et al., 2001). The initial stable isotopic composition of atmospheric CH_4 was modeled with a $\delta^{13}C_{CH_4}$ = −47.5 ‰ (VPDB), and $\delta^2H_{CH_4}$ = −100 ‰ (VSMOW) based on the work of Townsend-Small et al. (2012).

3. Results

Each of the 36 caves showed atmospheric to subatmospheric CH_4 concentrations in at least one location. Only five locations from three different caves showed elevated CH_4 concentrations relative to the surface atmosphere (Fig. 2, Supplemental Table 1). The CH_4 concentration in the surface atmosphere at study sites ranged from 1.8 ± 0.3 to 2.8 ± 0.7 ppmv. CH_4 concentrations in cave air ranged from ≤ 0.1 ± 0.1 ppmv to 5 ± 1 ppmv, and were generally observed to decrease with the distance from cave entrances (Fig. 3, Supplemental Table 1). Two thirds of the caves where three or more air measurements and distance data were recorded showed decreases in CH_4 concentration from cave entrances to interiors. For example, caves 7, 8, and 9 from Kentucky all showed progressive decreases in CH_4 concentration from about 2 ppmv at the entrance of the cave, down to zero or near zero ppmv in the more inner rooms (from 2 to 0 in caves 8 and 9 and from 1.9 to 0.3 ppmv in cave 7). Additionally, CH_4 concentrations were negatively correlated with CO_2 concentrations in cave air following an inverse power law relationship ($[CH_4] = 17.5[CO_2]^{-0.41}$, $r^2 = 0.26$) (Fig. 2). In the caves where Rn concentrations were measured, the average CO_2 concentration of cave air was correlated with the average Rn concentration of cave air ($[CO_2] = (1.42 \pm 0.09)[Rn] + 400 \pm 120$, $n = 4$, $r^2 = 0.99$, $p = 0.009$).

Values of $\delta^{13}C_{CO_2}$ in cave air ranged from −10.7 ± 0.4 to −23.81 ± 0.10 ‰. Analysis of $\delta^{13}C_{CO_2}$ values from samples with CO_2 concentrations above 600 ppmv showed that $\delta^{13}C_s$ ranging from −28 ‰ to −20 ‰ contributed to the composition of CO_2 in cave air. Pooled analysis of the CO_2 dataset shows that the average apparent source $\delta^{13}C_{CO_2}$ value is −23.3 ± 0.5 ‰ ($\delta^{13}C_{CO_2} = 4600\,[CO_2]^{-1} - 23.3 \pm 0.5$ ‰, $r^2 = 0.83$) (Fig. 4).

Values of $\delta^{13}C_{CH_4}$ and $\delta^2H_{CH_4}$ in cave air ranged from to -57.2 ± 0.6 to -27.1 ± 0.2 ‰ and -196 ± 10 to $+2 \pm 18$ ‰, respectively. Keeling plots of $\delta^{13}C_{CH_4}$ did not suggest that a two end member model was an adequate fit for the system ($\delta^{13}C_{CH_4}$ vs. $[CH_4]^{-1}$: $r^2 = 0.05$, $\delta^2H_{CH_4}$ vs. $[CH_4]^{-1}$: $r^2 = 0.12$). Some cave air samples plotted near the theoretical relationship between $\delta^{13}C_{CH_4}$ values and CH_4 concentrations caused by methanotrophy (Fig. 5). However, many points fell below and to the left of the line representing the theoretical incomplete oxidation of atmospheric CH_4 (Figs. 5, 6). When $\delta^2H_{CH_4}$ and $\delta^{13}C_{CH_4}$ values were plotted against each other, many samples clustered tightly near the signature of atmospheric CH_4 (Fig. 7). Some points, like those from caves 25 and 26, plotted near the expected trend of partial atmospheric CH_4 oxidation by methanotrophy. Other points plotted below or above this trend and indicated that at least two additional sources of CH_4 had to be entering the caves.

4. Discussion

4.1. Subsurface-Surface Atmospheric Exchange

The concentrations and stable isotopic compositions of CH4, CO2, Rn in cave air overlapped and diverged from those of the surface atmosphere. This suggests that atmospheric and cave processes influenced the composition of cave air. The atmospheric CH4 concentration at many study locations was above the globally averaged atmospheric background concentrations (1.87 ppmv CH4; Ciais et al., 2013) probably because they were near roads or pastures with local CH4 sources (Gioli et al., 2012; Harper et al., 2014). Rn concentrations were positively correlated with CO2 concentrations in cave air which agrees with other observations that have shown that CO2 concentrations in cave air track cave air residence time. The majority of cave air samples were depleted in CH4 and enriched in CO2 relative to the atmosphere, pointing to processes like in-situ CH4 oxidation and diffusion of air from the epikarst to decrease CH4 and increase CO2 concentrations (Fig. 2). Additionally, cave air CH4 concentrations generally decreased as the distance from an entrance increased (Fig. 3), and departures from this trend can be explained by fast airflow (caves 13, 25), cave air flowing out of the entrance (cave 26), multiple entrances resulting in multiple flow paths (cave 24), distance scales that were too small to observe a decrease in CH4 concentration (cave 20), or internal CH4 sources (cave 9). The patterns of CH4, CO2, and Rn concentration indicate that CH4 concentrations decrease with cave air residence time.

The concentration and stable isotopic composition of CO_2 in cave air show that in addition to an atmospheric end member, CO_2 with $\delta^{13}C_s$ values ranging from -28 to -20 ‰ were entering the caves and that the average source $\delta^{13}C_{CO_2}$ value was -23.3 ± 0.5 ‰ (Fig. 4). These observations generally agree with a CO_2 source from the soils and an atmospheric end-member. The $\delta^{13}C_{CO_2}$ values of many soils is near -24 ‰ (Amundson et al., 1998), and atmospheric $\delta^{13}C_{CO_2}$ values are frequently observed to be near -10 ‰ (Peyraube et al., 2013; Fernandez-Cortes et al., 2015). Due to fast airflow in cave 13 in Kentucky, the CO_2 concentration of 350 ± 6 ppmv and $\delta^{13}C_{CO_2} = -10.7 \pm 0.4$ ‰ in cave air were similar to the local background atmosphere (i.e. 400 ± 90 ppmv CO_2). It is possible that the observed source values that are more negative than -24 ‰ may be due to dripwater degassing or fast airflow (Spötl et al., 2005; Garcia-Anton et al., 2014). The $\delta^{13}C_s$ values that are more positive than -24 ‰ may be caused by differential abundances of C3 and C4 plants above the caves (Breecker et al., 2012). Our CO_2 data show that the caves in our study are not atypical compared to other caves in the literature and that cave air residence time increased as the $\delta^{13}C_{CO_2}$ values of cave air decreased.

4.2. Sources and Stable Isotopic Composition of Methane

Subatmospheric CH_4 concentrations in cave air suggest that CH_4 from the outside atmosphere is consumed in caves, and the addition of these observations to the existing datasets shows that karst is behaving as a sink for atmospheric CH_4 (Mattey et al., 2013; Ferndandez-Cortes et al., 2015; McDonough et al., 2016; Webster et al., 2016; Nguyễn-Thuỳ et al., 2017). Only three caves exhibited CH_4 concentrations above the atmospheric background, namely (i) cave 3, Indiana, (ii) cave 22, Tennessee, and (iii) cave 32, New Zealand. Caves with CH_4 concentrations above the atmospheric background appear to be uncommon, and understanding if there is a systematic change in karst landscapes from smaller order to higher order drainages awaits future work.

In some of the caves where we measured Rn concentrations, cave air flow was relatively fast. The average CO_2 and Rn concentrations from these caves were relatively low (cave 33, $[CO_2] = 540 \pm 20$ ppmv, $[Rn] = 20 \pm 100$ Bq m^{-3}; cave 34, $[CO_2] = 560 \pm 30$ ppmv, $[Rn] = 200 \pm 400$ Bq m^{-3}). Despite the similarity to atmospheric CO_2 concentrations in these caves, average CH_4 concentrations were still depleted relative to the atmosphere (cave 33, $[CH_4] = 1.07 \pm 0.06$ ppmv; cave 34, $[CH_4] = 1.34 \pm 0.06$ ppmv). These observations show that an *in-situ* process is removing CH_4 from the cave air because subatmospheric CH_4 concentrations in cave air are still observed in the absence of large increases in CO_2 concentrations as would be expected if CH_4 were only diluted by the arrival of CH_4-free air into caves from soils.

In several caves, values of $\delta^{13}C_{CH4}$ and δ^2H_{CH4} show that non-atmospheric $CH4$ enters caves because they were more negative than those predicted by the oxidation of atmospheric CH_4 via methanotrophy or reaction with ·OH. Other studies have also shown microbially produced CH_4 entering caves (Mattey et al., 2013; Webster et al., 2016). Our data point to the methanogenic sources of acetate fermentation and carbonate reduction (Fig. 7). Mixing between residual atmospheric CH_4 after partial methanotophic oxidation and CH_4 from acetate fermentation in the soil-epikarst-cave system will cause a decrease in the $\delta^{13}C_{CH4}$ and δ^2H CH_4 values of cave air compared to the atmospheric oxidation curve. Caves 23, 24, and 26 all appear to be influenced by acetoclastic methanogenesis. $CH4$ produced from carbonate reduction is inferred to enter the caves based on samples that had δ^2H_{CH4} values that were roughly equal to, or more positive than atmospheric values (Fig. 7). The stable isotopic compositions of $CH4$ from caves 5, 15, 25, and 27 can be explained by partial methanotrophic consumption of CH_4 generated from carbonate reduction with the strongest source signal in cave 5 (Fig. 7). $CO2$ reduction is typically observed in lake sediments, but has been observed in oxidizing environments such as biological soil crusts in deserts after rain events (Angel et al., 2011). We hypothesize that karst environments, which are less oxidizing, exhibit similar behavior. Our data show that carbonate reduction and acetate fermentation can occur in similar environments over large spatial scales and are not limited to arctic environments.

Sites of methanogenesis in or near the studied cave systems may include waterlogged soils above caves, cave soils themselves, and the epikarst. It is possible that after rain events anoxic micro niches occur in soil, the epikarst, or caves themselves and that the generated $CH4$ is dissolved and later introduced into caves with drip waters. We confirmed that dissolved $CH4$ outgasses in drip water of cave 32, which was situated underneath a wetland, by placing our $CH4$ detecting probe near the water and measuring increased $CH4$ concentrations in its vicinity. We confirmed that in-situ $CH4$ production can take place in locally anoxic environments within caves by measuring $CH4$ concentrations close to a bat guano deposit in cave 25, Tennessee (site 4h; average $CH4$ concentration = 0.3 ± 0.5 ppmv). Time series measurements near the large bat guano deposit showed that $CH4$ concentrations oscillated between 0.5 ppmv and 0.1 ppmv over the course of seconds, presumably in response to episodic migration of $CH4$ bubbles through the moist guano (similar oscillations in ammonia, $NH3$, were also observed). Additionally, we observed circumstantial evidence for local in-situ $CH4$ production in cave 3 because measured $CH4$ concentrations upstream of a restroom in the cave were low, while measured $CH4$ concentrations downstream of the restroom were enhanced. Our data show that caves are capable of expressing elevated $CH4$ concentrations

7

due to in-situ CH4 production when accumulations of organic matter, such as guano or plant material, foster methanogenesis or when dissolved CH4 from waters outgasses into cave air.

We observed minor amounts of thermogenic CH4 entering in at least one cave. Locally elevated CH4 concentrations in cave 9 (Mammoth Cave, Kentucky) were associated with a known hydrocarbon seep that is also transporting sulfide (Olson, 2013). Elevated CH4 concentrations, thought to derive from thermogenic CH4, have also been observed at sulfidic springs in Cueva de Villa Luz (Webster et al., 2017). Some δ13CCH4 and δ2HCH4 values in cave air, i.e. two of the samples from cave 24, are compatible with thermogenic CH4 isotopic signatures (e.g., Schoell, 1988; Etiope et al., 2009; Fig. 7). It cannot be excluded that small fluxes of CH4 from shales or hydrocarbon deposits underlying the limestone are entering caves through natural fractures, but our present isotope data cannot confirm this source for cave 24. The Antes and Utica shales, which contain hydrocarbon gases, are stratigraphically below cave 24 (Coleman et al., 2014), and geologic faults and joints, which are often aligned with caves, may serve as conduits for the flow of hydrocarbons (Powell, 1969; Koša et al., 2003). A confirmation of hydrocarbons entering from deep sources may be obtained through measurements of 'radiocarbon-dead' CO2, Rn, and ethane.

4.3. Methane Oxidation Mechanisms

The combination of $\delta^{13}C_{CH_4}$ and $\delta^2H_{CH_4}$ values allow for inferences to be made about how CH4 oxidizing reactions in karst environments. We distinguish between two scenarios with distinct sets of assumptions. Many isotopic compositions of CH4 in this study cannot be accounted for in the first scenario in which we assume that (i) CH4 enters the caves from the atmosphere, through acetate fermentation, and through carbonate reduction, and that (ii) CH4 is removed from cave air through reactions involving the ·OH. Conversely, in a second scenario, if it is assumed that (i) sources of CH4 in cave air include the atmosphere, acetate fermentation, and carbonate reduction, and that (ii) CH4 is removed from cave air by methanotrophy, all of the points fall within the plausibility envelope of the model, suggesting that methanotrophy is the mechanism responsible for removing CH4 from cave air (Fig. 7). Consideration of an additional source of thermogenic CH4 (natural gas) from deep geologic sources enlarges the plausibility fields of both prior scenarios to encompass all of the data. Our $\delta^{13}C_{CH_4}$ and $\delta^2H_{CH_4}$ data also agree with observations of $\delta^{13}C_{CH_4}$ and $\delta^2H_{CH_4}$ from a cave in Indiana where it appeared that CH4 from both acetate fermentation and carbonate reduction influenced cave air geochemistry (Webster et al., 2016). Additionally our data resemble an arctic system characterized by acetoclastic and hydrogenotrophic CH4 sources and methanotrophy (McCalley et al., 2014). Our isotopic evidence for *in-situ* microbial CH4 oxidation in caves is corroborated by recent results from *in-situ* mesocosm experiments in Vietnam where cave rocks with live microorganisms were shown to consume CH4 even in cases where surface soils were very thin to non-existent (Lennon et al., 2017; Nguyễn-Thuỳ et al., 2017).

5. Conclusions

Subterranean karst air generally shows subatmospheric CH4 concentrations. CH4 and CO2 concentrations were negatively correlated in cave air showing that as the residence time of cave air increases the CH4 concentration of cave air decreases. The stable isotopic composition of CH4 in studied caves suggests that CH4 is being oxidized by microbial methanotrophy. This evidence adds to earlier reports that methanotrophy is the mechanism by which CH4 is removed in cave air (Mattey et al., 2013; McDonough et al., 2016; Webster et al., 2016; Lennon et al., 2017). The observations of sub-atmospheric CH4

concentrations in cave air from this study and other studies shows that karst is behaving as a global sink for CH_4. CH_4 flux data from cave and karst landscapes are needed to estimate the size of the karst sink.

The stable isotopic composition of CH_4 in the studied caves suggests that, in addition to atmospheric CH_4, at least two additional CH_4 sources are present in some caves. We suggest that the sources include CH_4 produced from acetate fermentation and from CO_2 reduction. These data corroborate recent findings of partially oxidized CH_4 entering cave air from acetate fermentation and CO_2 reduction in Indiana (Webster et al., 2016). These observations of CH_4 production by acetate fermentation and carbonate reduction suggest that both processes happen over a wide scale in the environment.

Cave air CH_4 appears to have been isotopically shifted towards more positive $\delta^{13}C_{CH_4}$ and $\delta^2H_{CH_4}$ values due to methanotrophy in the soil-epikarst-cave system. Even though minor CH_4 production appears to be taking place in karst environments, CH_4 consumption is the dominant process.

Acknowledgements

References

1. Amundson, R., Stern, L., Baisden, T., Wang, Y., 1998. The isotopic composition of soil and soil-respired CO_2. Geoderma 82, 83–114. http://dx.doi.org/10.1016/S0016-7061(97)00098-0
2. Angel, R., Matthies D., Conrad, R., 2011. Activation of methanogenesis in arid biological soil crusts despite the presence of oxygen. PLoS ONE 6(5), e20453. http://dx.doi.org/10.1371/journal.pone.0020453
3. Batiot-Guilhe, C., Seidel, J.-L., Jourde, H., Hébrard, O., Bailly-Comte, V., 2007. Seasonal variations of CO_2 and ^{222}Rn in a Mediterranean sinkhole – spring (Causse d'Aumelas, SE France). International Journal of Speleology 36(1), 51-56.
4. Breecker, D.O., Payne, A.E., Quade, J., Banner, J.L., Ball, C.E., Meyer, K.W., Cowan, B.D., 2012. The sources and sinks of CO_2 in caves under mixed woodland and grassland vegetation. Geochimica et Cosmochimica Acta 96, 230-246. http://dx.doi.org/10.1016/j.gca.2012.08.023
5. Ciais, P., Sabine, C., Bala, G., Bopp, L., Brovkin, V., Canadell, J., Chhabra, A., DeFries, R., Galloway, J., Heimann, M., Jones, C., Le Quéré, C., Myneni, R.B., Piao, S., Thornton, P., 2013. Carbon and other biogeochemical cycles. *In* (Stocker, T.F., Qin, D., Plattner, G.-K., Tignor, M., Allen, S.K., Boschung, A., Nauels, A., Xia, Y., Bex, V., Midgley, P.M., eds.) Climate Change 2013: The Physical Science Basis. Contribution to Working Group I to the Fifth Assessment Report of the Intergovernmental

Panel on Climate Change. Cambridge University Press, Cambridge, United Kingdom and New York, NY, USA.

6. Coleman D.D., Risatti J.B., Schoell M., 1981. Fractionation of carbon and hydrogen isotopes by methane-oxidizing bacteria. Geochimica et Cosmochimica Acta 45(7), 1033-1037. http://dx.doi.org/10.1016/0016-7037(81)90129-0

7. Coleman, J.L., Jr., Ryder, R.T., Milici, R.C., Brown, S., 2014. Overview of the potential and identified petroleum source rocks of the Appalachian Basin, Eastern United States. *In* (Ruppert, L.F., Ryder, R.T., eds.) Coal and Petroleum Resources in the Appalachian basin; Distribution, Geologic Framework, and Geochemical Character: U.S. Geological Survey Professional Paper 1708, http://dx.doi.org/10.3133/pp1708G.13

8. Cunningham, K.I., LaRock, E.J., 1991. Recognition of microclimate zones through radon mapping, Lecheguilla Cave, Carlsbad Caverns National Park, New Mexico. Health Physics 61(4), 493-500.

9. Dlugokencky, E.J., Houweling, S., Bruhwiler, L., Masarie, K.A., Lang, P.M., Miller, J.B., Tans, P.P., 2003. Atmospheric methane levels off: Temporary pause or a new steady state? Geophysical Research Letters 30 (1992), http://dx.doi.org/10.1029/2003GL018126

10. Dlugokencky, E.J., Nisbet, E.G., Fisher, R., Lowry, D., 2011. Global atmospheric methane: budget changes, and dangers. Phil. Trans. R. Soc. A 369, 2058-2072. http://dx.doi.org/10.1098/rsta.2010.0341

11. Etiope G., Feyzullayev A., Baciu C.L., 2009. Terrestrial methane seeps and mud volcanoes: a global perspective of gas origin. Marine and Petroleum Geology 26, 333-344. http://dx.doi.org/10.1016/j.marpetgeo.2008.03.001

12. Feisthauer, S., Vogt, C., Modrzynski, J., Szlenkier, M., Krüger, M., Siegert, M., Richnow, H.-H., 2011. Different types of methane monooxygenases produce similar carbon and hydrogen isotope fraction patterns during methane oxidation. Geochimica et Cosmochimica Acta 75(5), 1173-1184. http://dx.doi.org/10.1016/j.gca.2010.12.006

13. Fernandez-Cortes, A., Cuezva, S., Alvarez-Gallego, M., Garcia-Anton, E., Pla C., Benavente, D., Jurado V., Saiz-Jimenez, C., Sanchez-Moral, S., 2015. Subterranean atmospheres may act as daily methane sinks. Nature Communications 6(7003). http://dx.doi.org/10.1038/ncomms8003

14. Garcia-Anton, E., Cuezva, S., Fernandez-Cortes, A., Benavente, D., Sanchez-Moral, S., 2014. Main drivers of diffusive and advective processes of CO_2-gas exchange between a shallow vadose zone and the atmosphere. International Journal of Greenhouse Gas Control 21, 113-129. http://dx.doi.org/10.1016/j.ijggc.2013.12.006

15. Ford, D., Williams, P., 2007. Karst Hydrogeology and Geomorphology. John Wiley & Sons Ltd, England.

16. Gioli, B., Toscano, P., Lugato, E., Matese, A., Migilietta, F., Zaldei, A., Vaccari, F.P., 2012. Methane and carbon dioxide fluxes and source partitioning in urban areas: The case study of Florence, Italy. Environmental Pollution 164, 125-131. http://dx.doi.org/10.1016/j.envpol.2012.01.019

17. Gregorič, A., Zidanšek, A., Vaupotič, J., 2011. Dependence of radon levels in Postojna Cave on outside air temperature. Natural Hazards and Earth System Sciences 11, 1523-1528. http://dx.doi.org/ 10.5194/nhess-11-1523-2011

18. Gregorič, A., Vaupotič, J., Šebela, S., 2014. The role of cave ventilation in governing cave air temperature and radon levels (Postojna Cave, Slovenia). International Journal of Climatology 34(5), 1488-1500. http://dx.doi.org/10.1002/joc.3778

19. Harper, L.A., Weaver, K.H., De Visscher, A., 2014. Dinitrogen and methane gas production during the anaerobic/anoxic decomposition of animal manure. Nutrient Cycling in Agroecosystems 100(1), 53-64. http://dx.doi.org/10.1007/s10705-014-9626-9

20. Hutchens, E., Radajewski, S., Dumont, M.G., McDonald, I.R., Murrell, J.C., 2004. Analysis of methanotrophic bacteria in Movile Cave by stable isotope probing. Environmental Microbiology 6(2), 111-120. http://dx.doi.org/10.1046/j.1462-2920.2003.00543.x

21. Jones, D.S., Albrecht, H.L., Dawson, K.S., Schaperdoth, I., Freeman, K.H., Pi, Y., Pearson, A., Macalady, J.L., 2012. Community genomic analysis of an extremely acidophilic sulfur oxidizing biofilm. The ISME Journal 6, 158-170. http://dx.doi.org/10.1038/ismej.2011.75

22. Kirschke, S., Bousquet, P., Ciais, P., Saunois, M., Canadell, J.G., Dlugokencky, E.J., Bergamaschi, P., Bergmann, D., Blake, D.R., Bruhwiler, L., Cameron-Smith, P., Castaldi, S., Chevallier, F., Feng, L., Fraser, A., Heimann, M., Hodson, E.L., Houweling, S., Josse, B., Fraser, P.J., Krummel, P.B., Lamarque, J.-F., Langenfelds, R.L., Le Quéré, C., Naik, V., O'Doherty, S., Palmer, P.I., Pison, I., Plummer, D., Poulter, B., Prinn, R.G., Rigby, M., Ringeval, B., Santini, M., Schmidt, M., Schindell, D.T., Simpson, I.J., Spahni, R., Steele, L.P., Strode, S.A., Sudo, K., Szopa, S., van der Werf, G.R., Voulgarakis, A., van Weele, M., Weiss, R.F., Williams, J.E., Zeng, G., 2014. Three decades of global methane sources and sinks. Nature Geoscience 6, 812-8123.

23. Keeling, R.F., Piper, S.C., Bollenbacher, A.F., Walker, S.J., 2010. Monthly atmospheric $^{13}C/^{12}C$ isotopic ratios for 11 SIO stations. *In* Trends: A Compendium of Data on Global Change. Carbon Dioxide Information Analysis Center, Oak Ridge National Laboratory, U.S. Department of Energy, Oak Ridge, Tenn., U.S.A.

24. Koša, E., Hunt, D., Fitchen, W.M., Bockel-Rebelle, M.-O., Roberts, G., 2003. The heterogeneity of paleocavern sytems developed along syndepositional fault zones: The Upper Permian Capitan Platform, Guadalupe Mountains, U.S.A. SEPM Special Publications No. 78 and APPG Memmoir 83, 291-322.

25. Kowalczk, A.J., Froelich, P.N., 2010. Cave air ventilation and CO_2 outgassing by radon-222 monitoring: How fast do caves breathe? Earth and Planetary Science Letters 289, 209-219. http://dx.doi.org/10.1016/j.epsl.2009.11.010

26. Lennon, J.T., Nguyễn-Thùy, D., Phạm, T.M., Drobniak, A., Tạ, P.H., Phạm, N.Đ., Streil, T., Webster, K.D., Schimmelmann, A., 2017. Microbial contributions to subterranean methane sinks. Geobiology 15(2), 254-258. http://dx.doi.org/10.1111/gbi.12214

27. Mattey, D.P., Fairchild, I.J., Atkinson, T.C., Latin, J.-P., Ainsworth, M., Durell, R., 2010. Seasonal microclimate control of calcite fabrics, stable isotopes and trace elements in modern speleothem from St. Michaels Cave, Gibraltar. *In* (Pedley, H.M., Rogerson, M. eds.) Tufas and Speleothems: Unravelling the Microbial and Physical Controls: Geological Society, London, Special Publications 336, 323-344. http://dx.doi.org/10.1144/SP336.17

28. Mattey, D.P., Fisher, R., Atkinson, T.C., Latin, J.-P., Durrell, R., Ainsworth, M., Lowry, D., Fairchild, I.J., 2013. Methane in underground air in Gibraltar karst. Earth and Planetary Science Letters 374, 71-80. http://dx.doi.org/10.1016/j.epsl.2013.05.011

29. McCalley, C.K., Woodcroft, B.J., Hodgkins, S.B., Wehr, R.A., Kim, E.-H., Mondav, R., Crill, P.M., Chanton, J.P., Rich, V.I., Tyson, G.W., Saleska, S.R., 2014. Methane dynamics regulated by microbial community response to permafrost thaw. Nature 514, 478-481. http://dx.doi.org/10.1038/nature13798

30. McDonough, L.K., Iverach, C.P., Beckman, S., Manfield, M., Rau, G.C., Baker, A., Kelly, B.F.J., 2016. Spatial variability of cave-air carbon dioxide and methane concentrations and isotopic compositions in a semi-arid karst environment. Environmental Earth Sciences 75(700), http://dx.doi.org/10.1007/s12665-016-5497-5

31. Miller, J.B., Mack, K.A., Dissly, R., White, J.W.C., Dlugokencky, E.J., Tans, P.P., 2002. Development of analytical methods and measurements of $^{13}C/^{12}C$ in atmospheric CH_4 from the NOAA Climate Monitoring and Diagnostics Laboratory Global Air Sampling Network. Journal of Geophysical Research: Atmospheres 107(D13), ACH 11-1-ACH 11-15. http://dx.doi.org/10.1029/2001JD000630

32. Nisbet, E.G., Dlugokencky, E.J., Manning, M.R., Lowry, D., Fisher, R.E., France, J.L., Michel, M.E., Miller, J.B., White, W.J.C., Vaughn, B., Bousquet, P., Pyle, J.A., Warwick, N.J., Cain, M., Brownlow, R., Zazzeri, G., Lanoisellé, M., Manning, A.C., Gloor, E., Worthy, D.E.J., Brunke, E.-G.,

Labuschagne, C., Wolff, E.W., Ganesan, A.L., 2016. Rising atmospheric methane: 2007-2014 growth and isotopic shift. Global Biogeochemical Cycles 30, 1356-1370. http:///dx.doi.org/10.1002/2016GB005406

33. Nguyễn-Thuỳ, D., Schimmelmann, A., Nguyễn-Văn, H., Drobniak, A., Lennon, J.T., Tạ, P.H., Nguyễn, N.T.Á., (2017). Subterranean microbial oxidation of atmospheric methane in cavernous tropical karst. *Chemical Geology*. https://doi.org/10.1016/j.chemgeo.2017.06.014

34. Olson, R., 2013. Potential effects of hydrogen sulfide and hydrocarbon seeps on Mammoth Cave ecosystems. Mammoth Cave Research Symposia. Paper 28. http://digitalcommons.wku.edu/mc_reserch_symp/10th_Research_Symposium_2013/Research_Posters/28

35. Palmer, A.N., 1991. Origin and morphology of limestone caves. Geological Society of America Bulletin 103(1), 1-21. http://dx.doi.org/10.1130/0016-7606(1991)103<0001:OAMOLC>2.3.CO;2

36. Peyraube, N., Lastennet, R., Denis, A., Malaurent, P., 2013. Estimation of epikarst air P_{CO_2} using measurements of water $\delta^{13}C_{TDIC}$, cave air P_{CO_2} and $\delta^{13}C_{CO_2}$. Geochimica et Cosmochimica Acta 118, 1-17. http://dx.doi.org/10.1016/j.gca.2013.03.046

37. Peyraube, N., Lastennet, R., Villanueva, J.D., Houillon, N., Malaurent, P., Denis, A., 2016. Effect of diurnal and seasonal temperature variation on Cussac cave ventilation using CO_2 assessment. Theoretical and Applied Climatology, http://dx.doi.org/10.1007/s00704-016-1824-8

38. Powell, R.L. 1969. Base level, and climatic controls of karst groundwater zones in South-Central Indiana. Indiana Academy of Science, 281-291.

39. Sarbu, S.M., Kane, T.C., Kinkle, B.K., 1996. A chemoautotrophically based cave ecosystem. Science 272(5270), 1953-1955. http://dx.doi.org/10.1126/science.272.5270.1953

40. Saueressig, G., Crowley, J.N., Bergamaschi, P., Brühl, C., Brennikmeijer, C.A.M., Fischer, H., 2001. Carbon 13 and D kinetic isotope effects in the reactions of CH4 with O(^{1}D) and OH: New laboratory measurements and their implications for the isotopic composition of stratospheric methane. Journal of Geophysical Research 106 (D19), 23127–23138. http://dx.doi.org/10.1029/2000JD000120

41. Schoell, M., 1988. Multiple origins of methane in the Earth, *in* Schoell, M. ed. Origins of Methane in the Earth. Chemical Geology 71, 1-10. http://dx.doi.org/10.1016/0009-2541(88)90101-5

42. Spötl, C., Fairchild, I.J., Tooth, A.F., 2005. Cave air control on dripwater geochemistry, Obir Caves (Austria): Implications for speleothem deposition in dynamically ventilated caves. Geochimica et Cosmochimica Acta 69(10), 2451-2468. http://dx.doi.org/10.1016/j.gca.2004.12.009

43. Sussman, R., Forster, F., Rettinger, M., Bousquet, P., 2012. Renewed methane increase for five years (2007-2011) observed by solar FTIR spectrometry. Atmospheric Chemistry and Physics 12, 4885-4891. http://dx.doi.org/10.5194/acp-12-4885-2012

44. Templeton, A., Chu, K.-H., Alvarez-Cohen, L., Conrad, M.E., 2006. Variable carbon isotope fractionation expressed by aerobic CH4-oxidizing bacteria. Geochimica et Cosmochimica Acta 70(7), 1739-1752. http://dx.doi.org/10.1016/j.gca.2005.12.002

45. Townsend-Small, A., Tyler, S.C., Pataki, D.E., Xu, X., Christensen, L.E., 2012. Isotopic measurements of atmospheric methane in Los Angeles, California, USA: Influence of "fugitive" fossil fuel emissions. Journal of Geophysical Research 117(D07308). http://dx.doi.org/10.1029/2011JD016826

46. Tu, K.P., Brooks, P.D., Dawson, T.E., 2001. Using septum-capped vials with continuous-flow isotope ratio mass spectrometric analysis of atmospheric CO_2 for Keeling plot applications. Rapid Communications in Mass Spectrometry 15(12), 952-956. http://dx.doi.org/10.1002/rcm.320

47. Weary, D.J., Doctor, D.H., 2014. Karst in the United States: A digital map compilation and database: U.S. Geological Survey Open-File Report 2014–1156. http://dx.doi.org/10.3133/ofr20141156

48. Webster, K.D., Mirza, A., Deli, J.M., Sauer, P.E., Schimmelmann, A., 2016. Consumption of atmospheric methane in a limestone cave in Indiana, USA. Chemical Geology 443, 1-9. http://dx.doi.org/10.1016/j.chemgeo.2016.09.020

49. Webster, K.D., Rosales Lagarde, L., Sauer, P.E., Schimmelmann, A., Lennon, J.T., Boston, P.J., 2017. Isotopic evidence for the migration of thermogenic methane into a sulfidic cave, Cueva de Villa Luz, Tabasco, Mexico. Journal of Cave and Karst Studies 79(1), 24-34. https://caves.org/pub/journal/PDF/V79/cave-79-01-24.pdf.

50. Whiticar, M.J., 1999. Carbon and hydrogen isotope systematics of bacterial formation and oxidation of methane. Chemical Geology 161, 291-314. http://dx.doi.org/10.1016/S0009-2541(99)00092-3
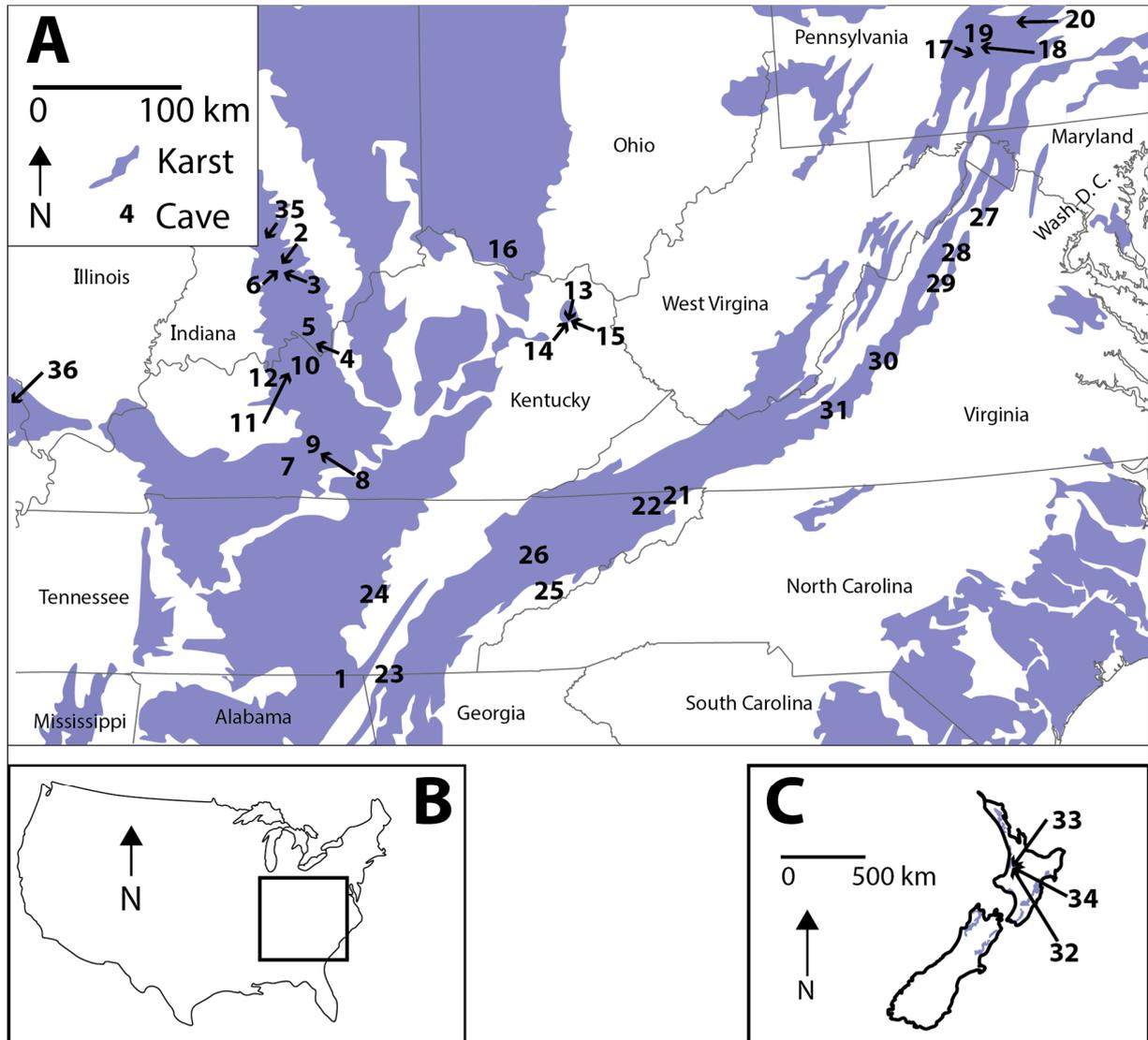
Figure 1. Locations of the U.S. study caves in their regional context (A) and within the contiguous USA (B). The location of the New Zealand caves are presented in C. Karst land cover data were obtained from Weary and Doctor (2014) and Ford and Williams (2007).
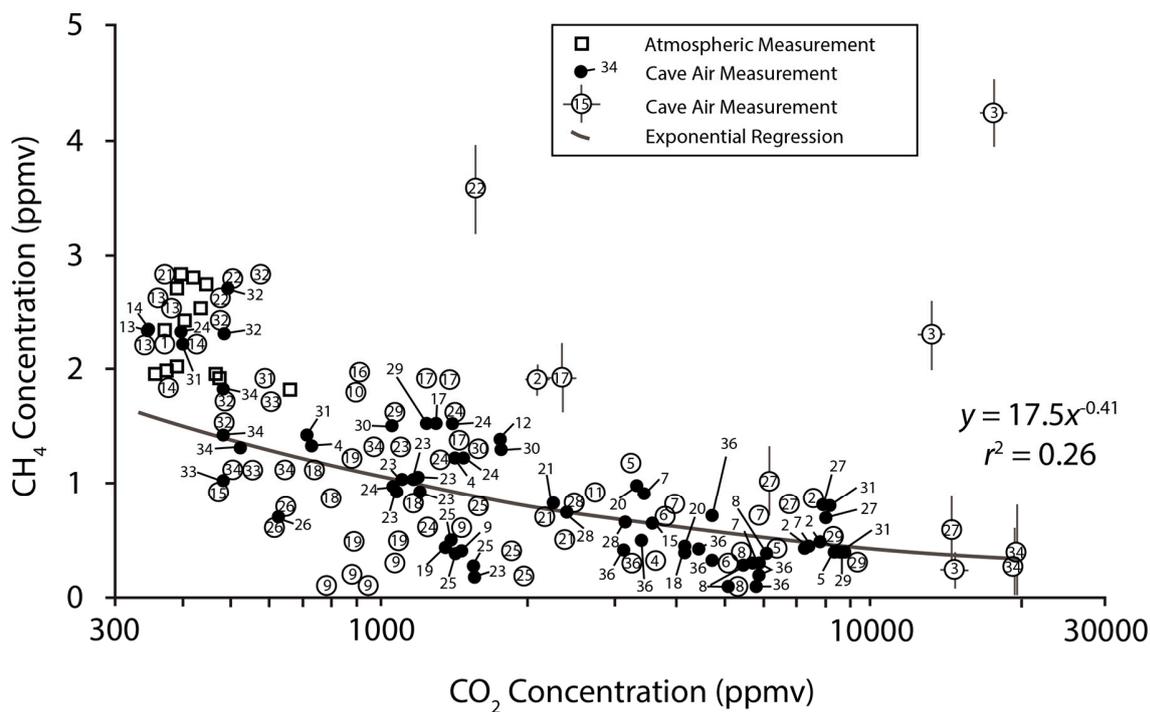
Figure 2. CH_4 concentrations *versus* CO_2 concentrations in studied caves. The majority of samples appear to follow an inverse power law relationship with CH_4 concentrations being inversely related to CO_2 concentrations (with points from caves 3 and 22 removed from the overall trend). Numbers represent individual caves. For clarity some error bars were omitted from the figure. Data associated with error bars are also representative for typical errors of data where no bars are shown.

Figure 3. The spatial variation of CH_4 mole faction in the air of cave 8, Kentucky. CH_4 concentration

dropped sharply from 1.5 to 0.5 ppmv along a narrow path after the first large room, a few tens of meter

from the entrance. CH_4 gradually decreased over roughly 100 m down to 0 ppmv in the Cathedral room.

Both the Inspectra (Gazomat, France assembled by West Systems, Italy) and the GasFinder2 (Boreal Laser

Inc., Spruce Grove, Alberta, Canada) use tunable diode lasers.

Figure 4. A Keeling plot of $\delta^{13}C_{CO_2}$ *versus* inverse CO_2 concentration in cave air samples. The data show

that atmospheric CO_2 is mixing with apparent isotopic endmembers between −33 and −20.4 ‰. A

regression analysis of the entire data set shows that the average $\delta^{13}C_{CO_2}$ value entering the caves is −23.3 ±

0.5 ‰. Numbers represent individual caves. Error bars are not included for clarity.
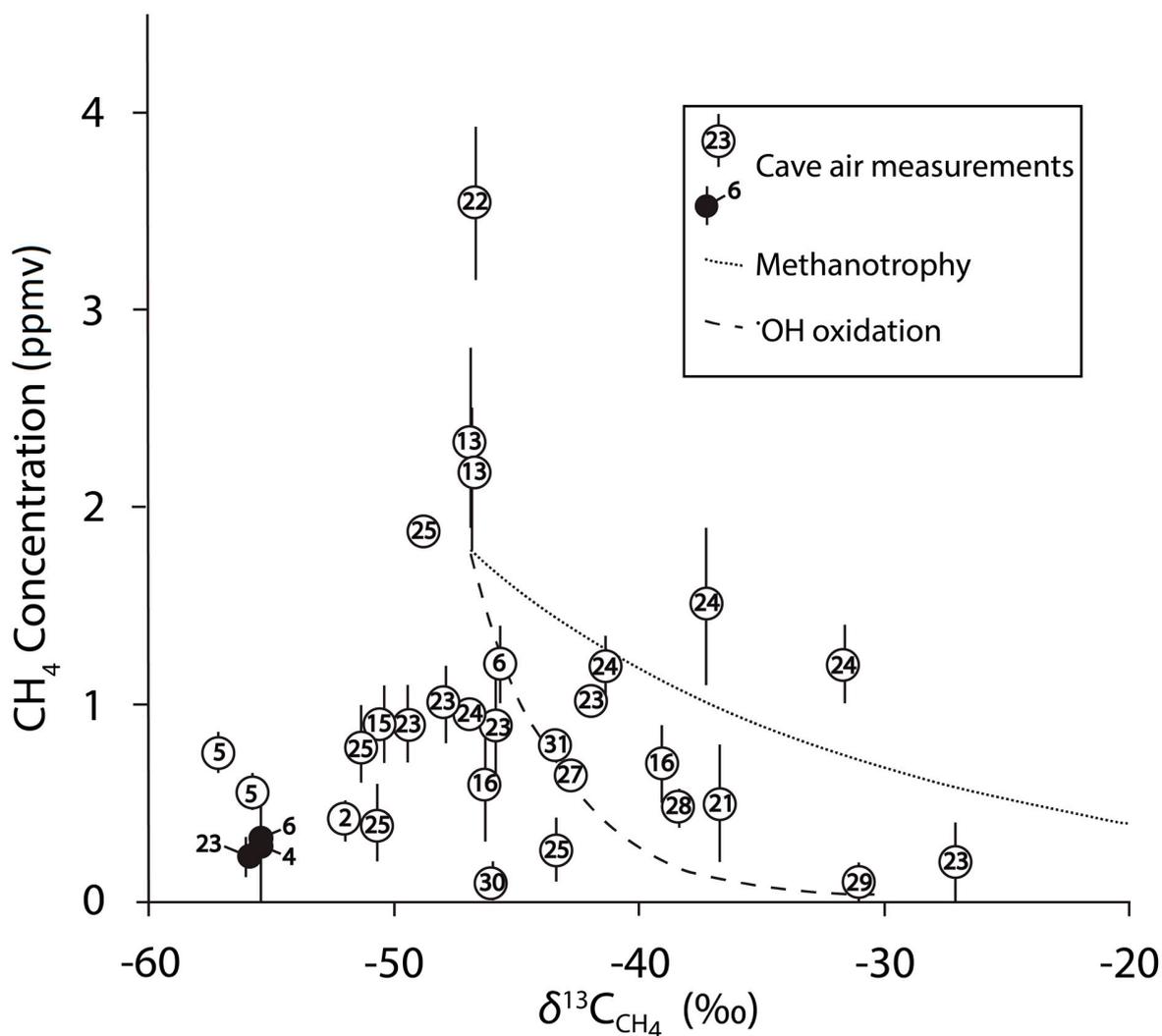
Figure 5. Relationship between CH_4 concentration and $\delta^{13}C_{CH_4}$ in cave air. Some samples plot along the

expected relationship between CH_4 concentration and $\delta^{13}C_{CH_4}$ caused either by methanotrophy modeled

with an α value of 1.018, or by oxidation with ·OH modeled with an α value of 1.0039. Other samples plot

below and to the left of the theoretical shifts of the oxidation trends. Numbers represent individual caves.

If error bars are not visible, they are smaller than the data points.
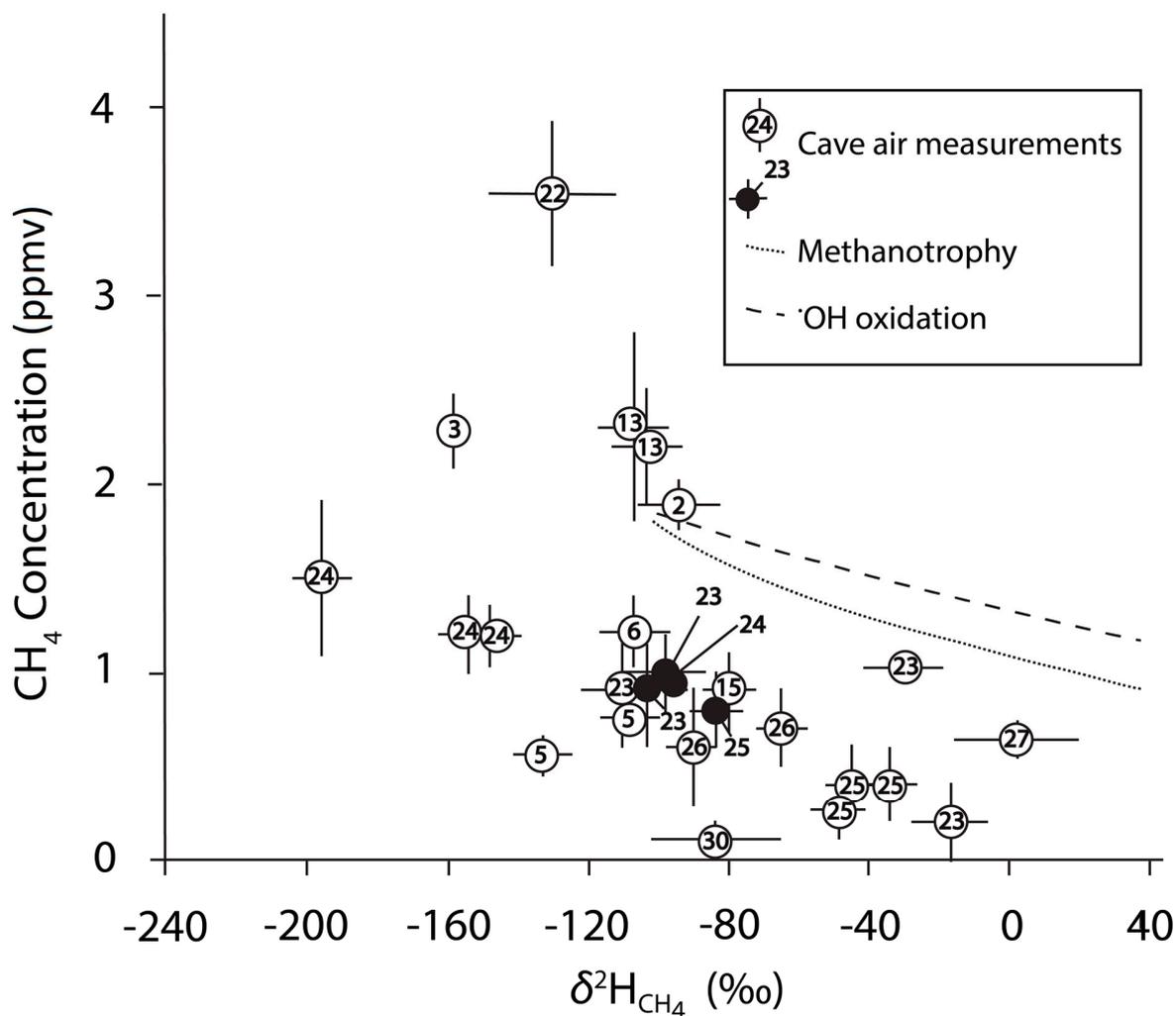
Figure 6. Relationship between methane concentration and $\delta^2 H_{CH_4}$ in cave air. Some samples plot along the expected relationship between CH_4 concentration and $\delta^2 H_{CH_4}$ caused by methanotrophy modeled with an α. value of 1.1353, or by oxidation with $\cdot OH$ modeled with an α.value 1.294. Other samples plot below and to the left of the shift caused by methanotrophy. Numbers represent individual caves. If error bars are not visible, they are smaller than the data points.
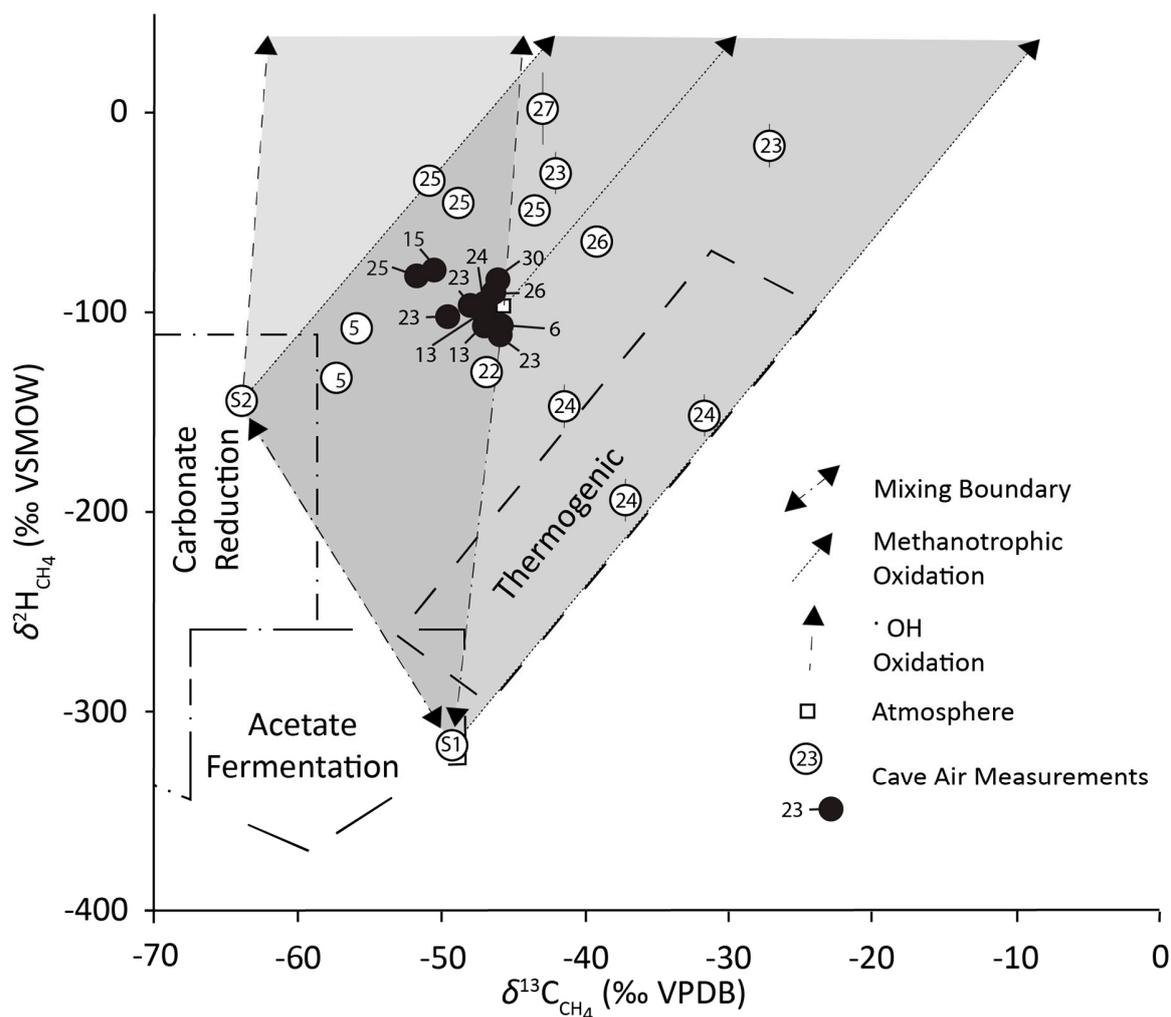
Figure 7. Stable isotopic composition of CH₄ in cave air samples plotted in $\delta^2 H_{CH_4}$ *versus* $\delta^{13} C_{CH_4}$ space.

CH₄ generated by carbonate reduction, acetate fermentation, and thermogenesis are plotted within

labeled fields (Whiticar, 1999). Dotted lines indicate the expected shift in $\delta^2 H_{CH_4}$ and $\delta^{13} C_{CH_4}$ caused by

partial aerobic methane oxidation adopting a slope of 8.5. Dashed lines indicate the expected shift in

$\delta^2 H_{CH_4}$ and $\delta^{13} C_{CH_4}$ caused by oxidation with ·OHadopting a slope 75 (Saueressig et al., 2001; Feisthauer et

al., 2011). Mixing in $\delta^2 H_{CH_4}$ vs $\delta^{13} C_{CH_4}$ space plots as a straight line. Numbers represent individual caves. If

the cave system can be characterized by sources from the atmosphere (□, −47.5 ‰, −100 ‰), acetate

fermentation (S1, −49 ‰, −325 ‰), and carbonate reduction (S2, −63 ‰, −125 ‰), and methanotrophy the

data should plot between the methanotrophic boundaries between S1 and S2, shaded in medium gray. If

the same sources are considered to be entering the cave and are oxidized by the ·OH radical they should

plot between the ·OH oxidized boundary of S1 and the atmosphere, and mixing between S1 and S2 as

well as mixing between S2 and the atmosphere, shaded light gray. Error bars are not included with black

circles for clarity. In other locations, if error bars are not visible, they are smaller than the data points.

Table 1: Overview of collected data. 'Discrete' measurements refer to the laboratory.

Cave	State	Collection date[a]	Sites measured	[CH$_4$] min (ppmv)	[CH$_4$] max (ppmv)	[CO$_2$] min (ppmv)	[CO$_2$] max (ppmv)	Methods
1	AL	2015-04-07	1	NA[b]	2.2	NA	378	*In-situ*
2	IN	2013-08-10	4	0.42	1.89	2140	8000	Discrete
3	IN	2013-08-07	3	0.23	4.2	13400	17900	Discrete
4	IN	2013-06-18	2	0.3	0.7	3900	5200	Discrete
5	IN	2013-06-29	3	0.4	1.18	3300	8600	Discrete
6	IN	2013-06-14	3	0.32	1.32	750	3700	Discrete
7	KY	2012-05-05	4	0.3	0.9	3500	6020	*In-situ*
8	KY	2012-05-06	5	0.1	0.4	5200	6200	*In-situ*
9	KY	2012-05-07	7	0.08	0.6	900	1500	*In-situ*
10	KY	2013-07-18	1	NA	1.79	NA	920	Discrete
11	KY	2013-07-18	1	NA	0.91	NA	2790	Discrete
12	KY	2013-07-18	1	NA	1.37	NA	1790	Discrete
13	KY	2015-04-10	4	2.3	2.6	349	390	Mixed
14	KY	2015-04-10	3	1.82	2.33	351	390	*In-situ*
15	KY	2015-04-10	2	0.9	1.8	440	486	Mixed
16	OH	2015-04-10	1	NA	1.95	NA	940	*In-situ*
17	PA	2013-07-15	5	1.4	1.9	1430	2400	Mixed
18	PA	2013-07-15	4	0.4	1.1	760	4250	Mixed
19	PA	2013-07-15	4	0.4	0.5	900	1400	Mixed
20	PA	2013-07-16	3	0.4	1.0	3390	4240	Mixed
21	TN	2013-07-18	3	0.5	1.25	2210	2430	Mixed
22	TN	2013-07-19	3	2.6	3.5	490	1610	Mixed
23	TN	2015-04-07	7	0.2	1.02	1100	1600	Mixed
24	TN	2015-04-08	6	0.6	1.6	1100	1515	Mixed
25	TN	2015-04-09	7	0.2	0.8	1430	2100	Mixed
26	TN	2015-04-09	3	0.6	0.79	630	660	Mixed
27	VA	2015-07-17	5	0.6	1.0	6300	14700	Mixed
28	VA	2015-07-17	4	0.4	0.8	2480	7600	Mixed
29	VA	2015-07-17	5	0.4	1.6	1100	8740	Mixed
30	VA	2015-07-18	5	0.3	1.5	1090	19900	Mixed
31	VA	2015-07-18	6	0.4	2.2	410	8900	Mixed
32	NZ[c]	2014-10-04	8	1.5	2.8	500	590	*In-situ*
33	NZ	2014-10-04	3	1.0	1.7	500	620	*In-situ*
34	NZ	2014-10-04	6	1.0	1.8	500	1000	*In-situ*
35	IN	2014-06-11	2	0.14	0.3	NA[d]	NA[d]	*In-situ*
36	MO	2016-09-24	9	0.1	1.5	2590	6190	*In-situ*

[a] Dates are formatted yyyy-mm-dd

[b] NA = not applicable where only 1 sample was obtained.

[c] NZ = New Zealand ,[d] NA = Only CH$_4$ was measured

Table 2: *In-situ* instrumentation used in this study.

Instrument	Maker	Location	Method	Analytes Measured	Lower detection limits
GasFinder2	Boreal Laser	Spruce Grove, Alberta Canada	Tunable Diode Laser Spectroscopy	CH_4	1 ppmv m^{-1}
Inspectra	Gazomat, WEST Systems	Pontedera, Italy	Tunable Diode Laser Spectroscopy	CH_4	0.1 ppmv
LGD F200	Axetris, SARAD	Kägiswil, Switzerland	Tunable Diode Laser Spectroscopy	CH_4	0.2 ppmv
madIR-D01 CO2	Madur, SARAD	Zgierz, Poland	Tunable Diode Laser Spectroscopy	CO_2	400 ppmv
DX4030	Gasmet	Milton Keynes, United Kingdom	Fourier Transform Infrared Spectroscopy	CH_4, CO_2, NH_3,	0.3 ppmv CH_4, 200 ppmv CO_2, 0.1 ppbv NH_3
LI820	LICOR, WEST Systems	Pontedera, Italy	Nondispersive Infrared Spectroscopy	CO_2	5 ppmv
RTM 2200	SARAD	Dresden, Germany	Alpha spectroscopy	Rn	0 Bq/m³